

## Simulation of Landfast Ice Along the Alaskan Coast

Mark A. Hopkins

US Army Cold Regions Research and Engineering Laboratory  
72 Lyme Rd., Hanover, NH 03755

June 2008

Final Report

MMS Interagency Agreement 0104RU35520



**U.S. Department of the Interior**  
**Minerals Management Service**  
**Alaska OCS Region**

# Simulation of Land Fast Ice Along the Alaskan Coast

Mark A. Hopkins

US Army Cold Regions Research and Engineering Laboratory  
72 Lyme Rd., Hanover, NH 03755

This study was funded by the U.S. Department of the Interior, Mineral Management Service (MMS), Alaska Outer Continental Shelf Region, Anchorage Alaska, under Interagency Agreement 0104RU35520, as part of the MMS Environmental Studies Program.

June, 2008.

This report has been reviewed by the Mineral Management Service and approved for publication. Approval does not signify that the contents necessarily reflect the views and policies of the Service nor does mention of trade names or commercial products constitute endorsement or recommendation for use.

## Table of Contents

Abstract	4
Introduction	4
High-Resolution Coastal Data Set	6
Preliminary Modeling Efforts	7
Parameterization of Sea Ice Ride-Up	8
Modeling Coastal Deformation	10
Acknowledgements	13
Literature Cited	13
Appendix: High-resolution Alaskan coastal data set	14

## Abstract

Sea ice modeling efforts have generally focused on ice dynamics and thermodynamics in the central pack that govern the large-scale motions and characteristics of the sea ice cover in the Arctic basin. These models have been coupled to ocean and atmospheric models to simulate the role of the Arctic pack in the global climate. Recently, because of the effects of climate change on the coastal environment, the prospect for a longer shipping season, and the rising costs of oil, interest has grown in modeling coastal ice conditions. However, it isn't at all clear that the Eulerian approach used in large-scale sea ice models can be carried into the landfast zone where coast lines and discontinuities between fast ice and pack ice are explicit, where individual features may span the entire area within the barrier islands, and where the required resolution may be so high that the continuum assumption fails. An alternative is to adopt a discontinuous Lagrangian approach and explicitly model ice parcels and the interactions between them. This work describes the steps that are necessary to develop a Lagrangian coastal sea ice model. Briefly, these steps are: development of a high-resolution data set to define the coastline, barrier islands, and man-made structures; development of a meshing strategy to increase model resolution in the coastal area coupled to a low-resolution basin scale model; parameterization of shore ride-up and grounded ridge formation processes; and lastly, a computational geometry algorithm that allows for floe destruction during compressive deformation. This last requirement remains incomplete and will be the focus of future efforts.

## Introduction

Over the last 20 years sea ice modeling has been focused on ice dynamics and thermodynamics in the central pack that govern the large-scale motions and characteristics of the sea ice cover in the Arctic basin. More recently these large-scale sea ice models have been coupled to ocean and atmospheric models to simulate the role of the Arctic pack in the global climate. These large-scale models of the Arctic pack take an Eulerian continuum approach that uses a plastic yield surface to characterize the constitutive behavior of the pack. The yield surface that is used is based on certain assumptions and represents averaged behavior over some representative area. It isn't at all clear that this approach can be carried into the landfast zone where coast lines and discontinuities between fast ice and pack ice are explicit, where individual features may span the entire area within the barrier islands, and where the required resolution may be so high that the continuum assumption fails.

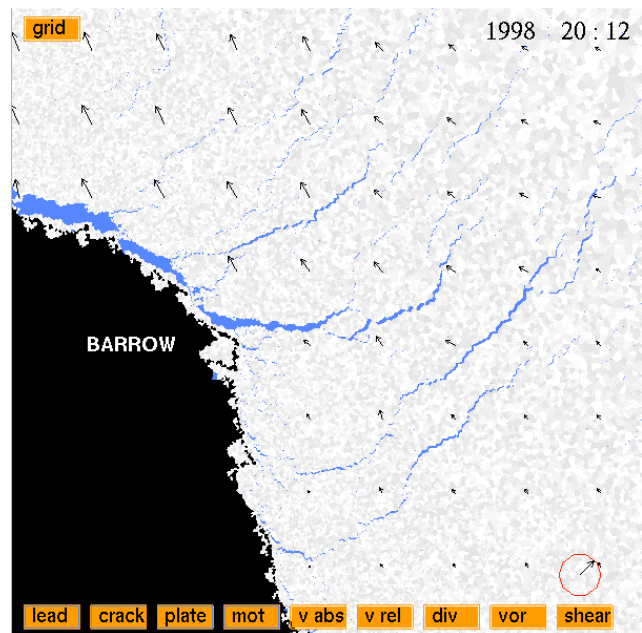


Figure 1. Showing leads in the model pack off Pt. Barrow. Vectors show ice velocity. 3 km resolution.

An alternative is to adopt a discontinuous Lagrangian approach and explicitly model ice parcels and the interactions between them. Over the last 10 years, with steady support from NASA spread over three projects, I have developed a Lagrangian model of the Arctic ice pack that consists of tens of thousands of individual floes (Hopkins, et al., 2004; Hopkins and Thorndike, 2006). Neighboring floes can freeze together to form plates. Plates can fracture to form smaller plates, diverge to form leads as shown in Figure 1, and converge to form ridges. In the model the fracture pattern created by deformation defines many large plates 10-100 km in width, shown in Figure 2, that are composed of aggregates of the small floes.

Subsequent deformation of the model pack takes place along the boundaries of the plates. Regional variations in the size of the plates correspond to regional variations in the gradient of the wind field and tensile strength between parcels (Hopkins et al., 2004). Secondary breakage can further reduce the size of the plates in response to external forces. Once the joint between two floes has broken they can diverge to form leads, converge to form pressure ridges, and slide along their boundaries. The discontinuities associated with leads and ridges are explicit. Pressure ridging is incorporated via a parameterization based on discrete element simulations of the ridging process (Hopkins, 1998). New ice is grown in open leads. Thermodynamic ice growth and ablation are simulated using a model developed by Flato and Brown (1996) in which each thickness category belonging to each floe has its own vertical temperature profile. Wind stress, temperature fields, and Coriolis accelerations drive the model pack. The simulation results are compared to basin-wide maps of divergence, vorticity, and shear produced by the Radarsat Geophysical Processor System (RGPS) (Kwok et al., 2001). The output of the model pack is run through a virtual RGPS processor to generate maps of LKFs for direct comparison with the RGPS. Regional variation of the basic floe size permits high resolution ( $< 1$  km) simulation of areas of interest.

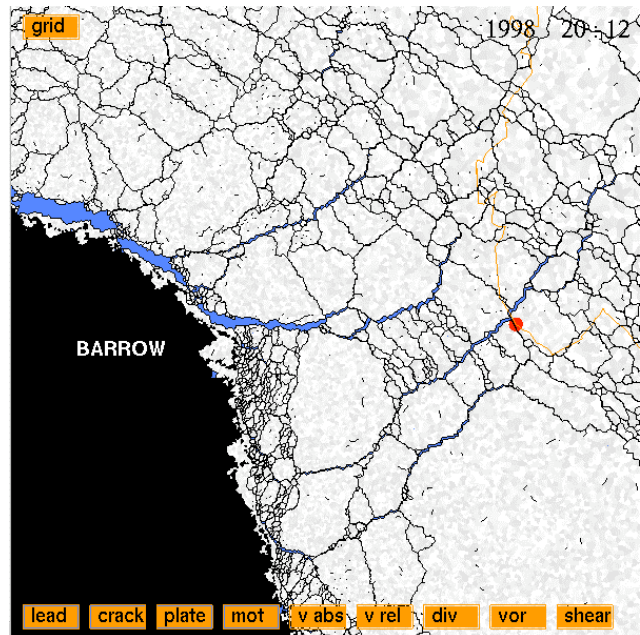


Figure 2. Showing the underlying crack pattern in the model pack in Figure 1. Note the landfast ice on the coast north of Pt. Barrow. (The orange line shows the drift path of the SHEBA experiment and the red dot shows the position on 1/20/1998.)

## High-Resolution Coastal Data Set

The discrete element based Lagrangian sea ice model consists of ice floe elements and boundary land elements. The coast line data sets used for basin scale simulations are typically >10 km resolution. With the requirement for sub-kilometer resolution in the coastal zone, it was necessary to develop a high-resolution coastal data set to define the coastal discrete elements. This was accomplished by Brian Tracy in the Remote Sensing and Geographic Information Systems Branch at CRREL. Tracy developed a data set working from RADARSAT imagery that has an average 70 m spacing between points extending from Wainwright west of Point Barrow to Barter Island near the Canadian border. An example RADARSAT image is shown in Figure 3. The data set is describe in the Appendix. The 70 m coastline data set was then interpolated to regular points 250 m apart. A section of the interpolated coastline is shown in Figure 4 below.



Figure 3. Radarsat image a section of the AK coast.

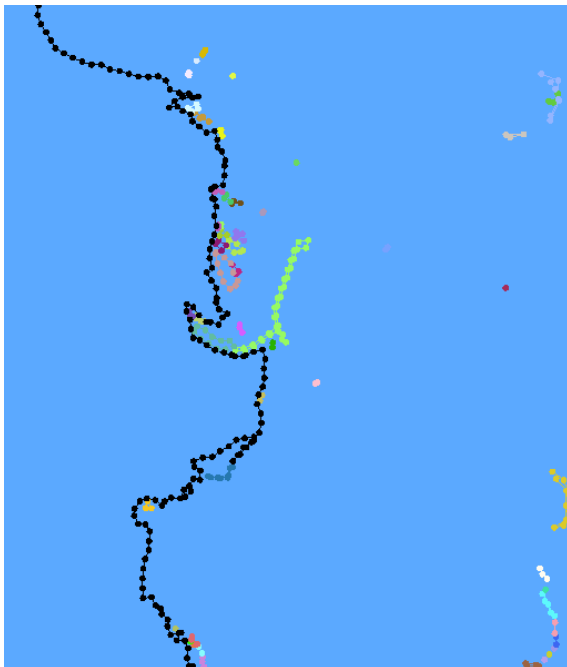


Figure 4. Showing the data points that define the coast, islands and causeway around Prudhoe, where each entity is delineated by a distinct color.

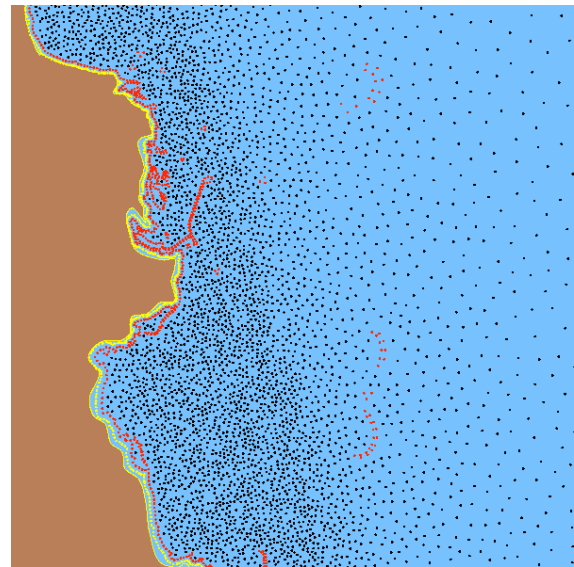


Figure 5. Showing the coastline (yellow) and islands (red) and the random seed points (black) used to define the centers of ice parcels. The resolution is 500 m near the coast and decreases with distance from the coast.

The high-resolution coast line for the Alaskan coast was combined with the 10 km Arctic basin coast line data set covering the remainder of the Arctic. Software was written to fill the basin with points that become centers of ice parcels in the model ice pack. Points were thrown randomly into the basin. The density of points was controlled by specifying a minimum distance between adjacent points. That is, when inserting a new point at a random location, the point had to be at least a minimum distance from its nearest neighbors. The point density in Figure 5 was varied linearly according to the distance from the Alaskan coast high-resolution area of interest. Near the coast the minimum distance between points was 500 m increasing linearly to 20 km over 200 km and remaining at 20 km over the rest of the basin. The ice floes were created using a Delaunay triangulation about the set of random points. The total number of points/floes in the basin was about 45000. Of these about half were in the near-coast area of interest shown in Figure 6.

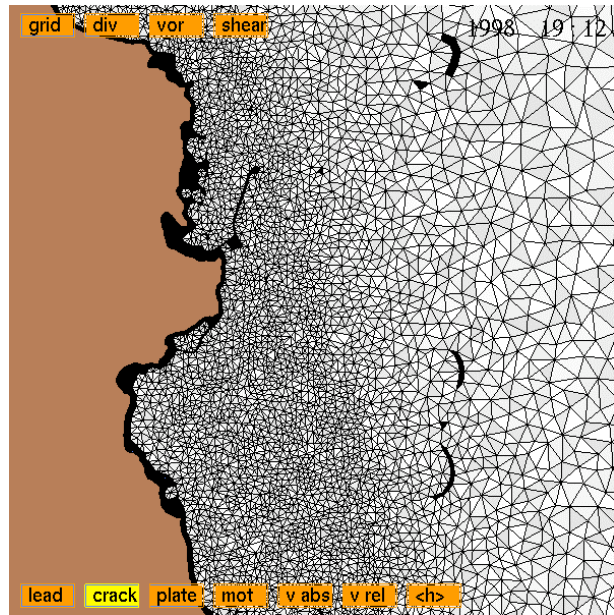


Figure 6. Showing the Delaunay triangulation of the model ice pack near Prudhoe constructed from the set of points in Figure 5. The resolution is 500 m near the coast and decreases with distance from the coast.

### Preliminary Modeling Efforts

The model ice pack described above was used to perform preliminary simulations. Three general wind forcing scenarios were tested in 24 hour simulations. Each simulation began using the same model ice pack. Three daily geostrophic wind fields were selected from the Navy Operational Global Atmospheric Prediction System (NOGAPS) (Zhang, et al., 1998) for January-February, 1998. The spatial and temporal resolution of the data was  $1^\circ \times 1^\circ$  and 24 hours, respectively. The first wind field was parallel to the coast on January 20, 1998. The second wind field was on shore on February 8, 1998. The third wind field was offshore on February 28, 1998. The three qualitatively different wind forcing scenarios produced three distinctly different fracture patterns in the nearshore sea ice. Figure 7 shows the fracture pattern produced by winds blowing parallel to the coast. Shear motion along the coast is composed of

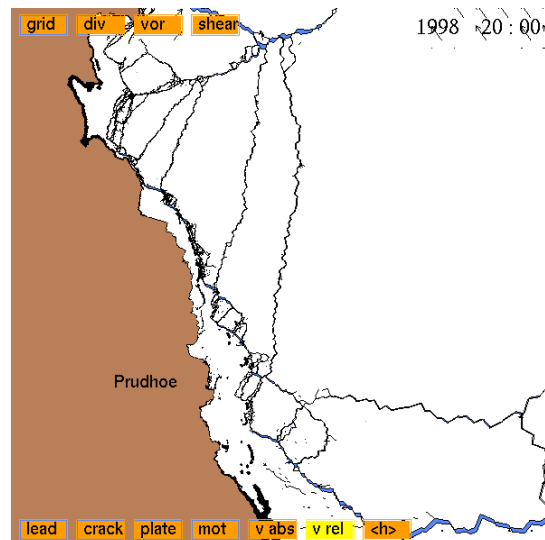


Figure 7. Deformation pattern created by winds blowing parallel to the coast.

alternating ridging and opening zones. Figure 8 shows the crack pattern produced by onshore winds. Onshore ice motion creates parallel ridging zones extending across the entire figure. Figure 9 shows the deformation pattern produced by offshore winds. This creates a much less complex crack pattern, significant opening and little or no ridging.

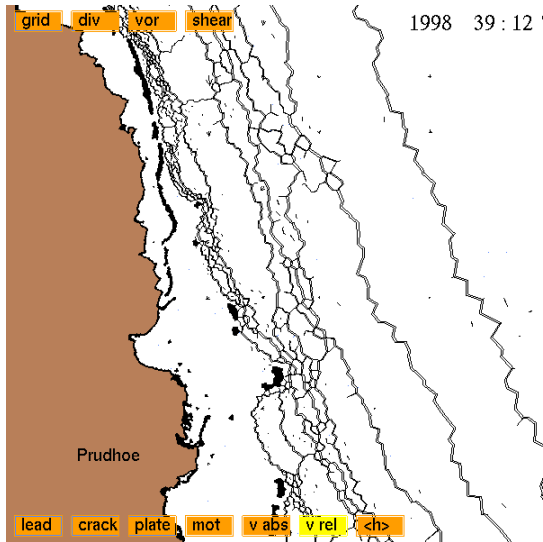


Figure 8. Deformation pattern created by onshore wind forcing.

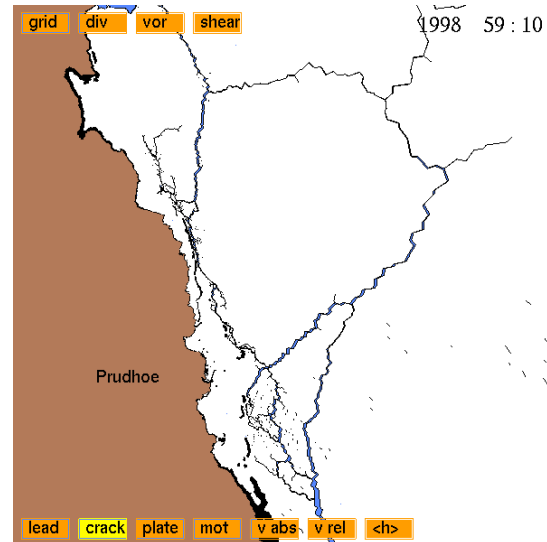


Figure 9. Deformation pattern created by offshore wind forcing.

### Parameterization of Sea Ice Ride-Up

To model coastal ice accumulation it was necessary to parameterize the grounded pressure ridging process. This entailed two significant tasks. The first was to develop a computer model of grounded ridge formation. The model is based on the successful central basin ridging model of Hopkins (1998) and the ride-up modeling of Hopkins (1997). In the model, grounded ridges are formed from a sheet of intact ice pushed against the shore. The seabed slopes upward toward the shore with a constant angle. Initial pile-up occurs on the shore. As the rubble accumulates the active ridging zone migrates seaward in the direction of the incoming sheet. The keel of the ridge will ground in shallow water. As the water deepens due to the sloping bed, more and more rubble will be required to ground the ridge. However, the sail height is limited by the strength of the parent ice sheet. This means that as the water deepens the buoyancy of the submerged grounded ridge will increase relative to the constant weight of the sail. Ultimately it is the difference between the weight of the sail and the buoyancy of the keel that keeps the ridge anchored. Figure 10 shows three scenes from a simulation; a close-up of the pile-up at the beach, a close-up of the grounded sea ward section, and a distant view of the entire grounded ridge.



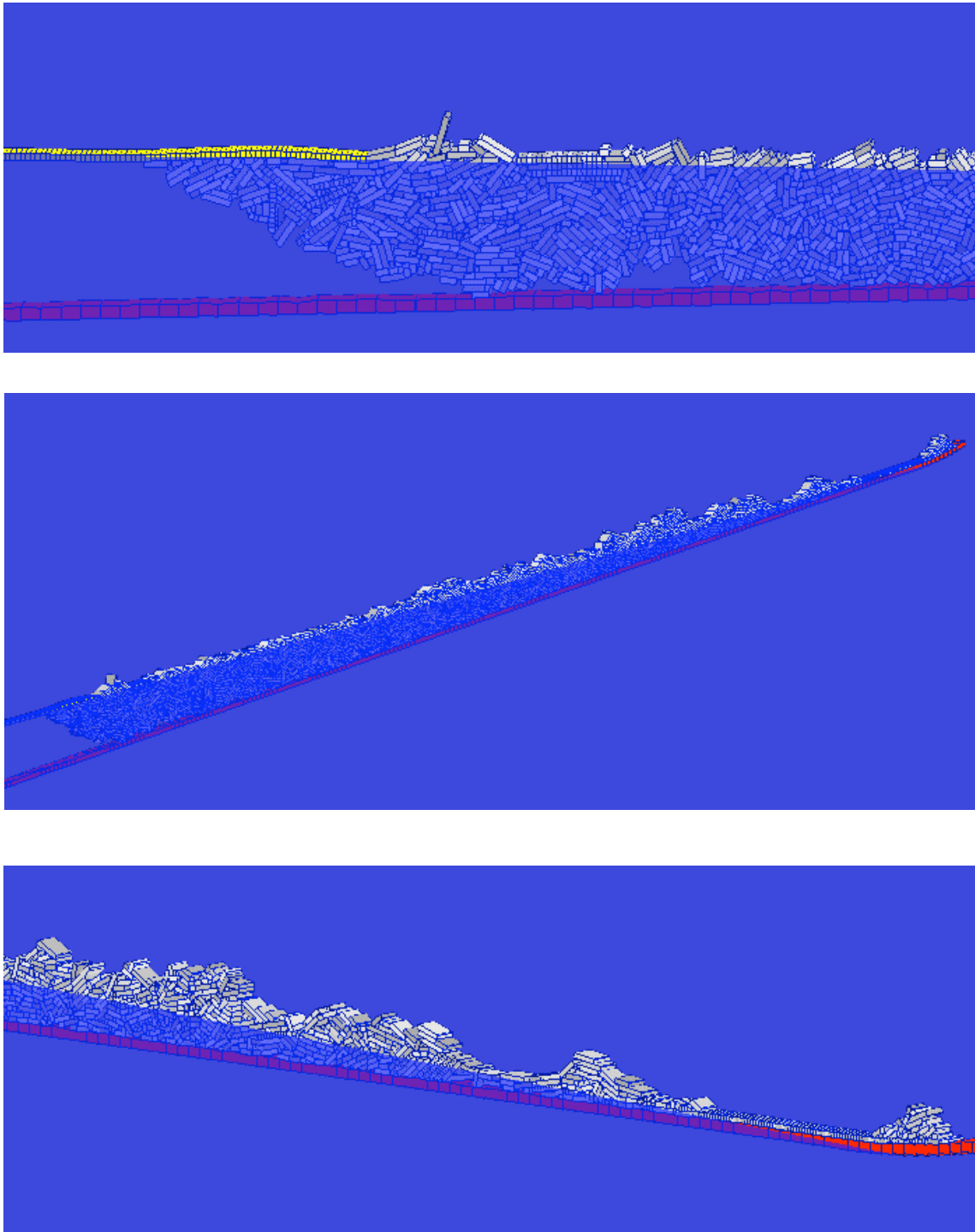


Figure 10. The three figures above show the beach end of the grounded ridge, the seaward end of the ridge, and the entire ridge. The parent ice thickness was 0.5 m and the maximum depth shown was 11 m. The sea bed is colored red, the intact sheet is yellow, and the blocks broken from the parent sheet are shaded gray.

The seaward extent  $L$  of the grounded ridge in terms of the length  $l$  of the parent ice pushed into the ridge is given by

$$L^2 + \frac{2h_s}{\tan\theta}L - \frac{h_i l}{(1-n)\tan\theta} = 0$$

where  $h_s$  is the average sail height,  $h_i$  is the thickness of the parent ice,  $\theta$  is the seabed slope (assumed constant), and  $n$  is the porosity of the ridged ice. The average sail height is assumed to depend on  $h_i$  and can be found in *Hopkins* (1998). This equation can be solved at each time step of the simulation in each grid cell adjacent to the coast to calculate the seaward progression of the edge of the grounded ridge. The forces are essentially the same forces calculated by *Hopkins* (1998) for first, second, and third stage pressure ridge formation. Grounded ridges very quickly reach the third stage when they have reached the maximum sail height for a given ice thickness  $h_i$  and then spread laterally in the direction of the oncoming sheet. The stage three ridging force in N/m is given by

$$F = 95400h_i^{3/2}$$

The parameterization of grounded ridge growth for seaward extent, keel depth and force has been incorporated into the high-resolution sea ice model. This will allow the model to simulate growth and stability of the landfast ice and stamuhki zone.

### Modeling Coastal Deformation

Compressive deformation of the ice in the near shore zone differs from the central Arctic pack in that floes are destroyed. In the central Arctic, forces are generally not sufficient to destroy a floe. However, in near shore areas ice floes are caught between the coastline and coastal sea ice driven by the integrated force of hundreds of kilometers of wind fetch. In other words, near shore ice is caught between an irresistible force and an immovable object. Under these conditions the ice floes in the near shore region may be completely destroyed by deformation and feed the formation of the extensive grounded ridge formations and rubble fields that line the near shore areas in much of the Arctic basin. The complete destruction of ice floes presents a rather severe challenge to the discrete, Lagrangian modeling approach being developed in this project.

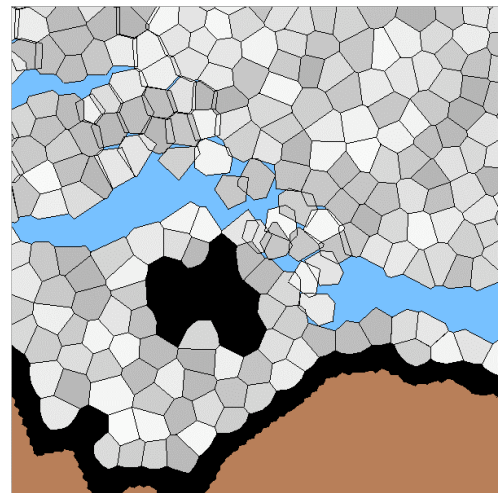


Figure 11. Showing the discrete polygons that compose the model ice pack. Coastline is black, land is brown, ice floes are shaded gray, and water is blue.

In the Lagrangian modeling approach the ice pack is composed of discrete ice floes as shown in Figure 11. When floes are pushed together in areas of convergence the polygons that make up the ice become overlapping. The overlapping areas are interpreted as ridged or rubble ice by the

constitutive relations used to calculate the ridging forces that resist further convergence. When a floe is entirely destroyed it completely overlaps other floes. At this point two difficulties crop up. First, the computational geometry algorithm used to calculate the overlap breaks down because the line of contact is indeterminate. Second, the subsequent motion of the floe is impossible to calculate because it can no longer interact with its surroundings. To overcome this problem I went back to the situation in the real pack where, although the floe is completely destroyed, its rubble still occupies some space. If we assume for the sake of discussion that ridging creates a rubble layer that is 5 times the thickness of the parent ice, then the area of rubble created when a floe is destroyed would be

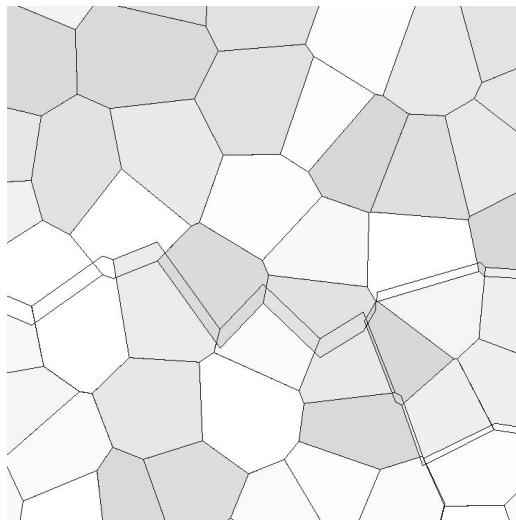


Figure 13. Showing a line of near shore ridged or overlapping floes.

$1/5$  the area of the original floe. So what we would like to create is an algorithm that keeps track of the fraction of rubble area and intact ice area in a deforming floe. Furthermore, the algorithm should reduce the size of the floe (and alter the shape) such that the area of the floe is equal to the sum of the area of rubble and intact ice in the floe. Thus, when the intact ice in the floe has been completely destroyed the floe (and its polygon) occupy  $1/5$  the space that it initially occupied.

The most difficult challenge that the development of this algorithm presents is that the shape of the polygon must be recalculated continuously as the polygon deforms, just as the shape of the real floe changes due to deformation. To develop the algorithm I used a simplified approach where a 100 km x 300 km rectangular model pack, shown in Figure 12, is pushed against a straight coast line by an onshore constant wind stress. The resolution varied from 5 km (bottom) to 500 m at the shore (top). I have developed this algorithm to a point where it is fairly robust. However, due to the geometric complexity of the intersecting polygons, shown in Figure 13, that continuously change during deformation and the difficulty of determining the line dividing two intersecting polygons, the algorithm occasionally breaks down. Unfortunately, in a DEM context

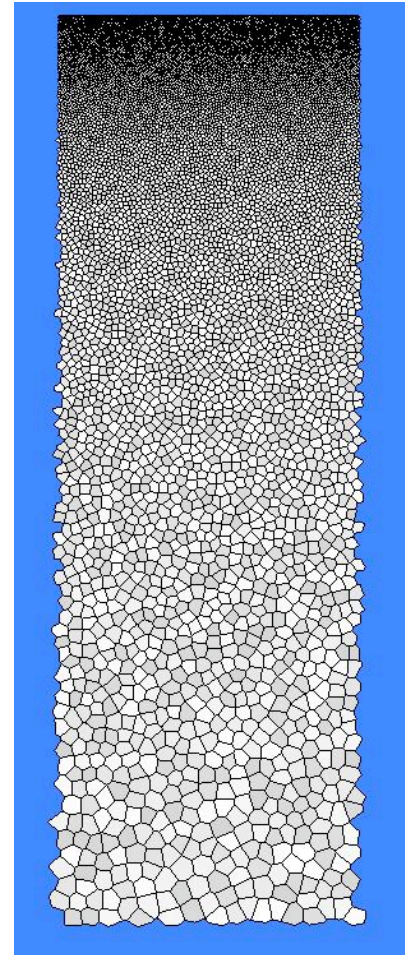


Figure 12. Linear onshore deformation model. Shore at top.

an algorithm must be utterly bulletproof or at least fail-safe. The algorithm needs more development before it is ready for inclusion in a production code. Until it is ready it is not possible to model the destruction of ice floes that routinely occurs in near shore areas.

The coastal ice ride-up model developed last year was compared to experiments in the CRREL refrigerated basin. The purpose of the experiments was to assess the ability of a rock revetment armor to withstand ice forces at Point Barrow. The full-scale model shown in Figure 14 reproduced the behavior seen in the 1:20 scale experiments. Unfortunately, no forces or other data were measured in the experiments.

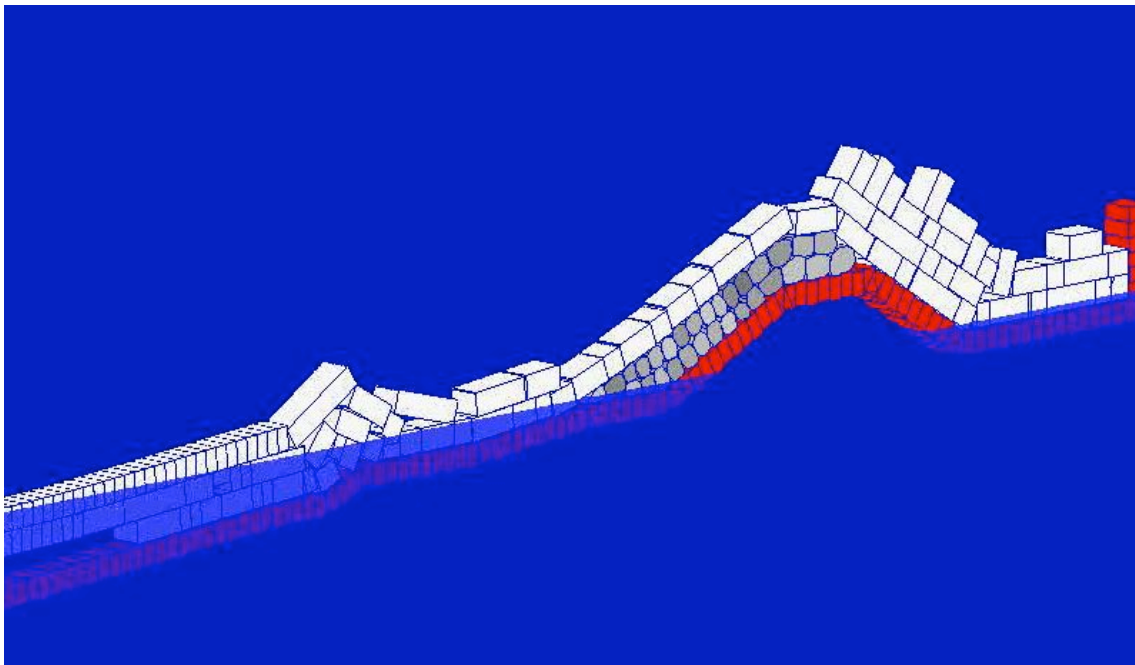


Figure 14. Showing ice ride-up on a proposed shore protection structure for Barrow, AK. Ice sheet thickness was 1.5 meters. The weight of the armor stones was 12 tons. The ground is colored red, the armor stones are shaded grey and the blocks broken from the parent sheet are white.

## Acknowledgements

The geostrophic wind fields used to drive the model were provided by the University of Washington Polar Science Center (Zhang et al., 1998).

## Literature Cited

Flato, G.M. and R.D. Brown (1996), Variability and climate sensitivity of landfast Arctic sea ice, *J. Geophys. Res.*, 101, (C10), 25767-25777.

Hopkins, M.A. (1997). Onshore ice pile-up: A comparison between experiments and simulations, *J. Cold Regions Science and Technology*, 26 205-214.

Hopkins, M.A., (1998). On the four stages of pressure ridging, *J. Geophys. Res.*, 103, (C10), 21883-21891.

Kwok, R., (2001). Arctic Ocean Sea Ice Deformation from SAR Ice Motion: Linear Kinematic Features, Jet Propulsion Lab Report, JPL D-21524.

Hopkins, M.A., S.F. Frankenstein, and A.S. Thorndike, (2004). Formation of an Aggregate Structure in the Arctic Ice Pack, *J. Geophysical Research*, Vol. 109, C01032.

Hopkins, M.A., and A.S. Thorndike (2006), Floe Formation in Arctic Sea Ice, *J. Geophysical Research*, Vol. 111, C11S23, doi:10.1029/2005JC003352.

Zhang, J., D.A. Rothrock, and M. Steele, (1998). Warming of the Arctic Ocean by a strengthened Atlantic inflow: Model results, *Geophys. Res. Lett.*, 25, 1745-1748.

## Appendix: High-resolution Alaskan coastal data set

With the requirement for sub-kilometer resolution in the coastal zone, it was necessary to develop a high-resolution coastal data set to define the coastal discrete elements. A data set was developed from RADARSAT imagery in the Remote Sensing and Geographic Information Systems Branch at CRREL. The points that define the coastline have an average spacing of 70 m. A plot of the data set is shown in Figure A1. The coastline defined by the data extends approximately from Wainwright, west of Barrow, to Barter Island near the Canadian border. The data set consists of points defined by a latitude and longitude. It is organized into 284 groups. The first group with 18868 points defines the coastline from north to south. Subsequent groups define the borders of offshore islands and structures. Each is a closed loop. The coastline is drawn arbitrarily across river mouths. The data is an ascii file organized in the following format:

```
# of groups
group 1, # of points in group 1
lat, long of points in group 1
...
...
group n, # of points in group n
lat, long of points in group n
```

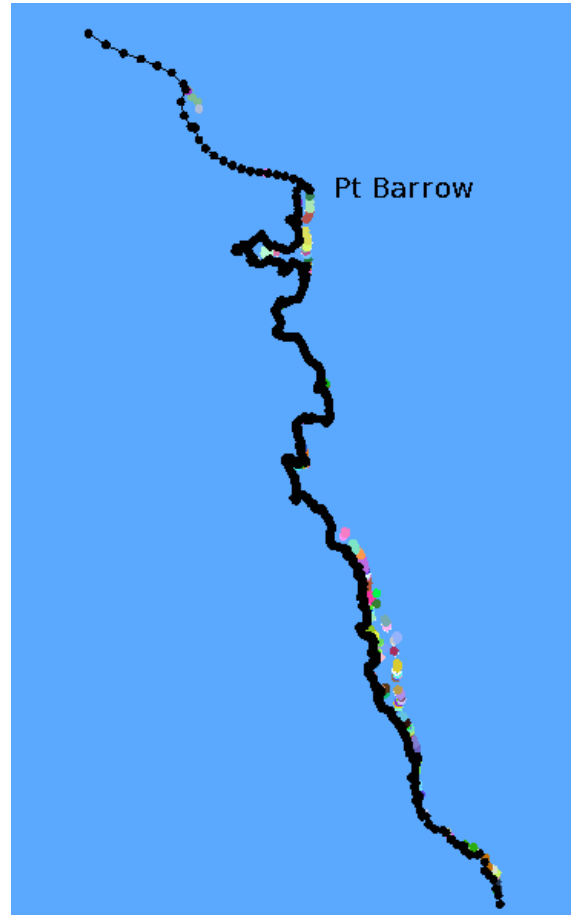


Figure A1. Showing the Alaskan coastline data set.



### The Department of the Interior Mission

As the Nation's principal conservation agency, the Department of the Interior has responsibility for most of our nationally owned public lands and natural resources. This includes fostering sound use of our land and water resources; protecting our fish, wildlife, and biological diversity; preserving the environmental and cultural values of our national parks and historical places; and providing for the enjoyment of life through outdoor recreation. The Department assesses our energy and mineral resources and works to ensure that their development is in the best interests of all our people by encouraging stewardship and citizen participation in their care. The Department also has a major responsibility for American Indian reservation communities and for people who live in island territories under U.S. administration.

### The Minerals Management Service Mission

As a bureau of the Department of the Interior, the Minerals Management Service's (MMS) primary responsibilities are to manage the mineral resources located on the Nation's Outer Continental Shelf (OCS), collect revenue from the Federal OCS and onshore Federal and Indian lands, and distribute those revenues.



Moreover, in working to meet its responsibilities, the **Offshore Minerals Management Program** administers the OCS competitive leasing program and oversees the safe and environmentally sound exploration and production of our Nation's offshore natural gas, oil and other mineral resources. The MMS **Royalty Management Program** meets its responsibilities by ensuring the efficient, timely and accurate collection and disbursement of revenue from mineral leasing and production due to Indian tribes and allottees, States and the U.S. Treasury.

The MMS strives to fulfill its responsibilities through the general guiding principles of: (1) being responsive to the public's concerns and interests by maintaining a dialogue with all potentially affected parties and (2) carrying out its programs with an emphasis on working to enhance the quality of life for all Americans by lending MMS assistance and expertise to economic development and environmental protection.